Biochimica et Biophysica Acta 1832 (2013) 46–56

Contents lists available at SciVerse ScienceDirect

Biochimica et Biophysica Acta

journal homepage: www.elsevier.com/locate/bbadis

FTIR spectroscopy: A new valuable tool to classify the effects of polyphenolic compounds on cancer cells

Allison Derenne [a], Vincent Van Hemelryck [a], Delphine Lamoral-Theys [c], Robert Kiss [b], Erik Goormaghtigh [a,*]

[a] Center for Structural Biology and Bioinformatics, Laboratory for the Structure and Function of Biological Membranes, Campus Plaine CP206/02, Université Libre de Bruxelles, Bld du Triomphe 2, CP206/2, B1050 Brussels, Belgium

[b] Laboratoire de Toxicologie, Toxicologie et Chimie Physique Appliquée; Faculté de Pharmacie, Université Libre de Bruxelles (ULB), Brussels, Belgium

[c] Laboratoire de Chimie BioAnalytique, Toxicologie et Chimie Physique Appliquée; Faculté de Pharmacie, Université Libre de Bruxelles (ULB), Brussels, Belgium

ARTICLE INFO

Article history:
Received 16 April 2012
Received in revised form 11 September 2012
Accepted 15 October 2012
Available online 23 October 2012

Keywords:
Polyphenol
IR spectroscopy
Cancer cell
IC_{50}

ABSTRACT

Polyphenolic compounds are an important part of human diet and regular consumption of fruits, vegetables and tea is associated with reduced risk of cancer. Dietary polyphenols display a vast array of cellular effects but the large number of data published in the literature makes it difficult to determine the main mechanisms of action associated and to identify molecules with original mechanisms. Therefore, there is an increasing demand for more systemic approaches in order to obtain a global insight of the biochemical processes mediated by polyphenols. Here, we used Fourier transform infrared (FTIR) spectroscopy to analyze cancer cells exposed *in vitro* to 6 polyphenols: 3 natural well documented polyphenols (curcumin, epigallocatechin gallate (EGCG) and quercetin) and 3 synthetic molecules with a very closely related chemical structure. Statistical analyses on FTIR spectra allowed the comparison of global effects of the 6 compounds and evidenced some common or different features in the cell perturbations among natural and synthetic molecules. Interestingly, marked metabolic changes induced by polyphenols closely related from a chemical point of view were identified. Furthermore, many metabolic changes could be detected as early as after 2 h incubation with the drugs.

1. Introduction

Polyphenolic compounds constitute one of the largest and most ubiquitous group of plant metabolites [1–3]. In nature, they are produced to protect plants from photosynthetic stress, reactive oxygen species, wounds and herbivores [1–3]. Although all plant phenolic compounds arise from amino acids phenylalanine and tyrosine, their structures are extremely diverse and they can be divided in at least ten classes based on their chemical structures [1–3].

Natural polyphenols are an important part of human diet and regular consumption of fruits, vegetables and tea is associated with reduced risk of cancer [4–6]. In addition, many epidemiological studies have demonstrated that food habits play a major role in the prevention of many human cancers [7]. Curcumin, for example, has been used for centuries in Asian countries and epidemiological data indicate that curcumin may be responsible for the lower rate of colorectal cancer in these countries [8]. An inverse association was also observed between lung cancer risk and the consumption of onions, apples, or white grapefruits as well as the calculated total intake of quercetin [9]. Likewise, several studies in Japan and China suggest that green tea consumption is associated with lower incidence of different types of cancer (gastric, breast, esophageal) [1,5]. The increasing mass of *in vitro* and *in vivo* scientific data relating to the chemopreventive and therapeutic effects of polyphenols in cancer has even stimulated clinical trials in order to address the pharmacokinetics, efficacy and safety of quercetin, EGCG and curcuma in humans [10].

Dietary polyphenols display a vast array of cellular effects and can affect all stages of carcinogenesis by up- or down-regulating multiple key proteins involved in diverse signal transduction pathways such as regulation of cellular proliferation, differentiation, apoptosis, angiogenesis or metastasis (see Table 1). However, the molecular pathways associated with the anticancer effects of polyphenols are dependent on the particular molecule studied, on the concentrations used in the various assays and on the cell types or tissues [10]. As a consequence, it becomes very difficult to compare and classify these compounds according to the change of one specific metabolite or the expression level of one particular protein.

Systemic approaches including metabolomics and proteomics seem promising in order to acquire a global insight in the biological and physiological processes mediated by polyphenols [4]. In this article, we suggest that the use of Fourier transform infrared (FTIR) spectroscopy-related analyses of cancer cells exposed *in vitro* to various types of polyphenols could provide a global signature of all the metabolic changes induced by these polyphenols.

Abbreviations: IR, infrared; FTIR, Fourier transform infrared; h, hour; S/N, signal to noise; SD, standard deviation; PCA, principal component analysis; PC, principal component; MANOVA, multivariate analysis of variance; ESS, error sum of square

* Corresponding author. Tel.: +32 2 650 53 86; fax: +32 2 650 53 82.
E-mail address: egoor@ulb.ac.be (E. Goormaghtigh).

0925-4439/$ – see front matter © 2012 Elsevier B.V. All rights reserved.
http://dx.doi.org/10.1016/j.bbadis.2012.10.010

Table 1
Modulation of cellular antioxidant status and of molecular signals involved in apoptosis, cell proliferation, inflammation, angiogenesis and metastasis induced by the 3 natural polyphenols used in this article. The arrow indicates an increase (↑), a decrease (↓) or no change (=) in the levels, phosphorylation status or activity of different signals. In certain cases, opposing results have been observed since experiments were carried out in different conditions (cell types, dose and time of treatment) [2–5,7,10,12,54].

Polyphenols	Modulation of cellular antioxidant status	Induction of cell cycle arrest	Induction of apoptosis	Inhibition of proliferation and inflammation	Inhibition of angiogenesis	Inhibition of metastasis
Curcumin		↓ Cyclin A; ↓ CDK1; ↑ p21; ↑ Cdc2	↑ caspase-3; ↑ caspase-7; ↑= caspase-8; ↑ caspase-9; ↑ AIF; ↑ cleaved PPAR; ↓ wm; ↓= Bcl-xL	↓ AKT; ↓ mTOR; ↓ p70S6K1; ↓ 4E-BP-1; ↓ IGF-I; ↓ NFκB; ↓ IKK; ↓ IκB; ↓ COX-2; ↓ PGE2		↓ MMP-1; ↓ MMP-2
EGCG	↓ H_2O_2-induced apoptosis; ↑ H_2O_2 production; ↑ ROS; ↑ GSH; ↓ Nrf-2-mediated HO-1 activation	↓= cyclin D; ↓= cyclin E; ↓ CDK1; ↓= CDK2; ↓ CDK4; ↓ CDK6; ↓ PCNA; ↑ p 16; ↑ p18; ↑= p21; ↑= p27; ↑ pRb; ↑ p53; = mdm	↑ ROS; ↑ caspase-3; ↑ caspase-8; ↑ caspase-9; ↑ cytochrome *c*; ↑ Smac/DIABLO; ↑↓= Bax; ↑ Bak; ↑ cleaved PPAR; ↓↑ Bcl-2; ↓= Bcl-xL; ↓ Bid; ↓ c-myc; = c-IAP1; ↓ c-IAP2; ↓ Mcl-1; ↓= survivin; ↓= XIAP	↓ PI3K; ↓↑= AKT; ↓↑ ERK; ↓ p90RSK; ↓ FKHR; ↓ PDGF; ↓ PDGFRb; ↓ EGFR; ↓↑ c-fos; ↓ egr-1; ↓ AP-1; ↓ NFκB; ↓ IKK; ↓ COX-2; ↑= JNK; ↑ Ras; ↑ MEKK1; ↑ MEK3; ↑↓ p38; ↑ IκB; ↑ AMPK; ↑ PGE2; ↑ TNF-a	↓ HIF-1a; ↓ VEGF; ↓ VEGFR1; ↓ VEGFR2	↓ MMP-2; ↓ MMP-9; ↓ FAK; ↓ proMMP-2; ↓ MRLC;
Quercetin	↓ CYP1A1; ↓ lactate dehydrogenase (LDH); ↑↓ GSH; malondialdehyde (MDA); ↓ ROS; ↓ GPx; ↓ SOD; ↓ GR; ↓↑ CAT; ↓ H_2O_2-induced apoptosis; ↑ QR; ↑ Nrf-2; ↓ Keap1; ↑ NQO1	↑ p53	↑ Caspase-3; ↑ caspase-7; ↑ caspase-8; ↑ caspase-9; ↑ cytochrome *c*; ↑= Bax; ↑ cleaved PPAR; ↓ ROS; ↓ wm; ↓= Bcl-2;	↓ PI3K; ↓↑= AKT; ↓↑ ERK; ↓ PKCa; ↓ EGFR; ↓ Erb2R; ↓ Erb3R; ↓↑ JNK; = PKCb; = PKCd	↓ VEGF; ↓ VCAM1; ↓ I-CAM1	↓ FAK; ↓ MMP-2; ↓ MMP-9

In the current work we have thus made use of an FTIR approach to analyze the effects contributed by three natural (curcumin, EGCG (epigallocatechin gallate) and quercetin) versus three synthetic (**13a**, **13b**, **13c**) polyphenols (Fig. 1) [11]. The three natural polyphenols display distinct chemical structures (Fig. 1) and display large numbers of already identified mechanisms possibly related to anticancer action (Table 1). Curcumin (diferuloylmethane) is extracted from the dried rhizome of *Curcuma longa* [8,12]. EGCG is the most common catechin found in green tea [5,13]. Quercetin (3, 3′, 4′, 5, 7-pentahydroxyflavone) is one of the most common flavonoids and is ubiquitously present in fruits and vegetables such as onion, tea, apples and berries [7,14]. In contrast, the three synthetic polyphenols are very closely related in terms of chemical structures, e.g. all three being trivanillates with minor chemical substitutions (Fig. 1). The *in vitro* effects of these six polyphenols were monitored by means of FTIR analyses in the human T98G glioblastoma cell line that displays resistance to pro-apoptotic stimuli [15,16] like human glioblastomas in clinical situations [17]. Glioma patients are associated with dismal prognoses because glioma cells resist conventional radiotherapy and chemotherapy [18]. Various polyphenols now appear as promising drugs to combat glioma cells [19–23].

2. Materials and methods

2.1. Cell culture

The human T98G glioblastoma cell line (CRL-1690) was obtained from the American Type Culture Collection (ATCC, Manassas, VA). T98G cells were incubated at 37 °C in sealed (airtight) Falcon plastic dishes (Cellstar, Greiner Bio-one, Wemmel, Belgium) in a humidified atmosphere of 5% CO_2. The cells were kept in exponential growth in RPMI medium supplemented with 10% fetal bovine serum (FBS), 2% penicillin/streptomycin (an antibiotic/antimycotic solution). Cell culture medium, FBS and antibiotics were purchased from Lonza (Verviers, Belgium). The mean duplication time of T98G cells is 23 ± 1 h, the 24 h growth rate is 172 ± 14% (100% is the number of cells in the first image, at 0 h), the 48 h growth rate is 372 ± 8% and the 72 h growth rate is 682 ±

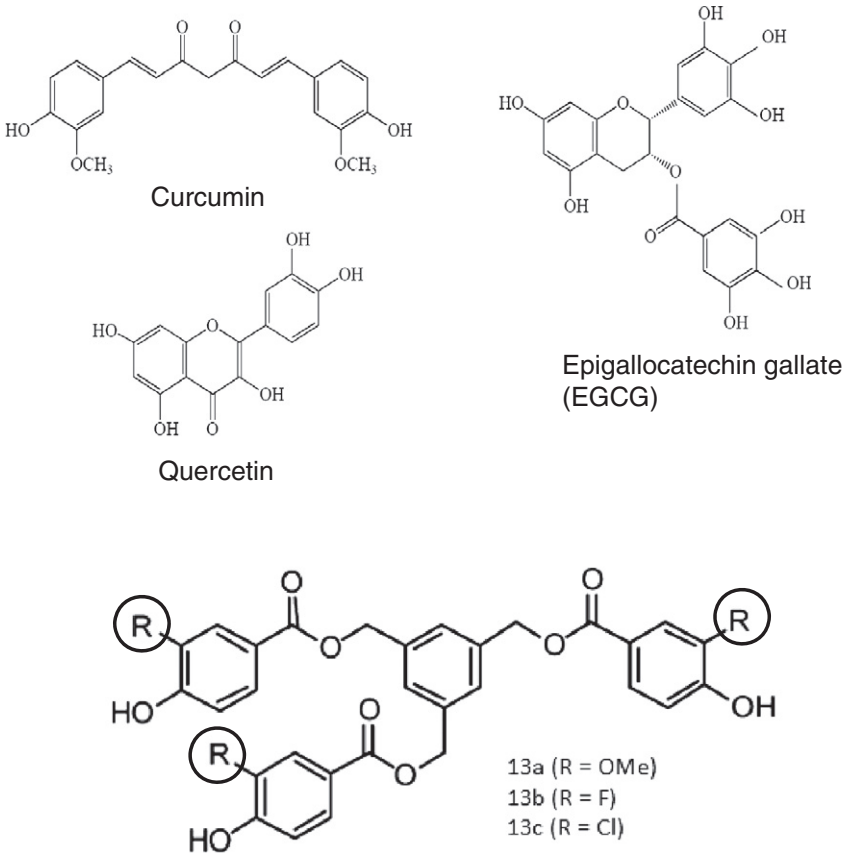

Fig. 1. Structure of the 6 polyphenolic compounds used in this study.

25%. These data were calculated on the basis of computer-assisted phase-contrast microscopy (quantitative videomicroscopy) enabling an image of the same T98G cell culture to be digitized every 4 min during 72 h. Duplication time of T98G cells has been calculated on sextuplicates at 24 h post cell plating. The growth rates have been calculated at the 24th, 48th and 72nd hour post cell plating. Cell cultures were tested for mycoplasma infection each 2 weeks using PlasmoTest from InvivoGen (Toulouse, France).

2.2. Determination of IC_{50} growth inhibitory concentrations

Drug concentrations used throughout this work are the IC_{50} concentrations defined as the drug concentration required for decreasing the global growth of a given cell population by 50% after 72 h of cell culture in the presence of the drug. IC_{50} concentrations were calculated by means of the MTT (3-[4,5-dimethylthiazol-2yl]-diphenyltetrazolium bromide, Sigma, Bornem, Belgium) colorimetric assay as detailed elsewhere [18,23,24] and briefly summarized as follows. T98G glioma cells were seeded in 96-microwell plates with an initial number of 1000 cells per well. Cells were then incubated for 24 h to ensure adequate cell adhesion before treatment. After this initial step, the various polyphenols were assayed from 10 nM up to 100 μM for 72 h and T98G cell population growth in control and polyphenol-treated conditions was determined according to the capability of living cells to reduce the MTT yellow product into the formazan blue product by a reaction occurring in the mitochondria [24,25]. Thus, the number of living cells after 72 h of culture in the presence (or the absence: control) of the various compounds is directly proportional to the intensity of the blue color, which is quantitatively measured by spectrophotometry—in our case using a Biorad Model 680XR (Biorad, Nazareth, Belgium) at 570 nm (with a reference of 630 nm). Each experiment was carried out in sextuplicate.

2.3. FTIR spectroscopy

For the FTIR spectroscopy, T98G cells were exposed to the six polyphenols at their respective IC_{50} concentrations for 2, 6 and 24 h. Before harvesting the cells, the medium was thrown away and cells were quickly washed with 1 ml trypsin (0.5 g/l)/EDTA (0.2 g/l) buffer (Lonza, Verviers, Belgium). So, if dead cells were present, they floated in the medium and were thus eliminated. Then, T98G cells were detached from their culture support by means of a 5-minute treatment with 1 ml trypsin (0.5 g/l)/EDTA (0.2 g/l) buffer (Lonza, Verviers, Belgium). The reaction was stopped by adding 1 ml of culture medium. The cells were pelleted by a 2-minute centrifugation (300 *g*), and washed three times in isotonic solution (NaCl, 0.9%) to ensure complete removal of trypsin and culture medium; they were then resuspended in around 10 μl of the NaCl solution.

Three independent cultures were grown for each condition and three samples were taken from each culture for infrared measurement, thus generating a total of nine spectra per condition. For the early incubation times (2 and 6 h), the experiment was independently repeated three times. For late incubation time (24 h), the experiment was independently carried out twice.

All measurements were carried out on a Bruker Equinox 55 FT-IR spectrometer (Bruker, Karlsruhe, Germany) equipped with a liquid N2-refrigerated mercury cadmium Telluride detector. All spectra were recorded by attenuated total reflection (for a review, see [26]). A diamond internal reflection element was used on a Golden Gate Micro-ATR from Specac (Orpington, UK). The angle of incidence was 45°. Around 0.5 μl of the resuspended cell was deposited on the diamond crystal (about 3×10^4 cells per smear) using a pipette (0.5–10 μl). The sample was quickly evaporated in N_2 flux to obtain a homogenous film of whole cells, as ascertained previously by microscope examination [27,28]. FTIR spectra were recorded between 4000 and 800 cm^{-1}. Each spectrum

was obtained by averaging 256 scans recorded at a resolution of 2 cm^{-1}. Values of maximal absorbance were always between 0.2 and 0.4 A.U.

2.4. Data analyses

All spectra were preprocessed as follows. Water vapor contribution was subtracted as described previously [29,30] with 1956–1935 cm^{-1} as reference peak. The spectra were then baseline-corrected and normalized for equal area between 1582 and 1492 cm^{-1} (Amide II peak). To subtract baselines, straight lines were interpolated between the point of the spectrum at the following wavenumbers: 3620, 2995, 2800, 2395, 2247, 1765, 1724, 1586, 1480, 1355, 1144, and 950. Then, they were subtracted from the spectrum.

The spectra were also smoothed at a final resolution of 4 cm^{-1} by apodization of their Fourier transform by a Gaussian line. Finally, signal/noise (S/N) was systematically checked on every spectrum. It was required to be greater than 450 when noise was defined as the standard deviation in the 2000–1900 cm^{-1} region of the spectrum and the signal is the maximum of the curve between 1750 and 1480 cm^{-1} after a baseline passing through these two points had been subtracted.

Normality of the distribution of the absorbances was checked for each group at every wavenumber by a Kolmogorov–Smirnov test by comparison with a standard normal distribution, with a confidence level $\alpha = 0.5\%$ (not shown). The results demonstrated the normality of absorbance distributions. For each culture run in the presence of a polyphenol, an additional culture of cells, free of any treatment, was grown in parallel and analyzed. These untreated cells were first used as control for the quality of the cultures. If the IR spectra of a control displayed any statistically significant differences ($\alpha = 0.5\%$) with previous controls, the entire experiment was repeated. Second, untreated cell spectra provided us with the reference FTIR fingerprint. Overall, around 100 nontreated cell spectra were recorded.

In IR spectra, each wavelength is a variable, i.e., about 1000 wavelengths are associated with biological molecule absorptions. With at least nine spectra for each condition, the number of variables submitted to statistical analysis quickly becomes extremely large. Data are best handled after principal component analysis (PCA), which is an unsupervised statistical method that enables a reduction of variables by building linear combinations of wavenumbers that vary together [31]. Diagonalization of the covariance matrix of the data provides new variables, the so-called principal components (PC) holding all the correlated original variables on which original spectra are finally projected. The first principal component accounts for most of the variance present in the data set; the second is built with the residual variance and is uncorrelated to the first one. The subsequent components are constructed in the same way and account for the residual variance. In practice, almost all the variance of the original data can be explained with five or six first PC, reducing the description of each spectrum to five or six numbers. Simultaneously, these weights allow an unsupervised classification of the spectra as such an observation does not suppose any a priori condition on these groups [31]. In the analyses reported here, the collection of spectra was mean-centered (the mean was removed from the individual spectra). Whether a group is significantly different from the others can be tested by multivariate analysis of variance (MANOVA) where each spectrum is identified by its projection on the first 6 principal components [32].

Ward's linkage is a method allowing hierarchical clustering of n groups with minimum loss of information. It is based on the similarity of group members with respect to many variables [33]. The grouping is based on the error sum of square criterion (ESS). At each step of the grouping procedure, each possible union is considered and the two items with the lower ESS are grouped. The process is repeated until the number of groups is reduced from n to 1 [34].

Correction of the spectra, Kolmogorov–Smirnov, Student *t*-tests, PCA, confidence ellipse, MANOVA and hierarchical classification were carried out by Kinetics, a custom made program, running under Matlab 7.1. (Matlab, Mathworks Inc.).

3. Results

3.1. IC_{50} growth inhibitory concentrations

The IC_{50} values relating to each of the six polyphenols under study with respect to T98G glioma cells are provided in Table 2. Typical dose–response curves for 2 molecules (13c and curcumin) are presented in the supplementary data (Fig. 6). These IC_{50} concentrations have been used for all FTIR analyses. The data in Table 2 show that the six polyphenols under study display relatively similar IC_{50} concentrations that range between 10 μM (curcumin) and 37 μM (**13b**). Thus, the determination of these IC_{50} concentrations did not reveal any clear distinction between these six polyphenols.

3.2. FTIR spectra of T98G cells treated with polyphenols

FTIR analyses rely on cell populations grown at 80% of confluence as defined elsewhere [35]. In the current experiment, T98G glioma cells were treated by six polyphenols (at their IC_{50} growth inhibitory concentration, see Table 2) for 2, 6 and 24 h. Between 18 and 27 FTIR spectra were recorded for each experimental condition. Fig. 2 displays the mean spectra (solid lines) and standard deviation (dotted lines) calculated at every cm^{-1} for cells incubated with the drugs indicated in the margins. Second derivative mean spectra for all the incubation time are presented in the supplementary data (Fig. 7). In Fig. 2 as well as in Fig. 7, very few changes are visible at first glance. Statistical analyses are thus applied to compare the six treatments at each of the three experimental times in order to evidence similarities versus differences in these spectra.

3.3. Cluster analyses

In order to better evidence spectral variations induced by each of the polyphenols at each of the three experimental times, the mean spectra of untreated cells (controls) was subtracted from the mean spectra of treated cells in each experimental condition. We thus obtained the "difference spectra", which are related to the actual metabolic modifications caused by each polyphenol in each experimental condition with respect to untreated T98G glioma cells. To compare and classify the six polyphenols at each of the three experimental times (2, 6 and 24 h), a hierarchical classification of the difference spectra was built. It must be emphasized that hierarchical clustering is an unsupervised method based on distance between spectra. Classification was performed on three spectral ranges: 3000–2800 cm^{-1}, 1800–1700 cm^{-1} and 1600–1000 cm^{-1}. The region between 1700 and 1600 cm^{-1} was avoided as it is usually disturbed by small variations in the water content of the sample.

Fig. 3 reveals that the three trivanillic polyphenols (**13a**, **13b** and **13c**) remain clustered when analyzed after 2 and 6 h, while at 24 h **13a** clusters with quercetin and EGCG, and curcumin clusters with **13b** and **13c**. It must be further noticed that the shape of the clusters

Table 2
IC_{50} of the 6 polyphenols used in this work. Concentration of drug reducing cell growth by 50% after 72 h (IC_{50}) for the six drugs used in this work.

Molecule	IC_{50} (μM)
13a	28
13b	37
13c	25
Curcumin	25
EGCG	10
Quercetin	30

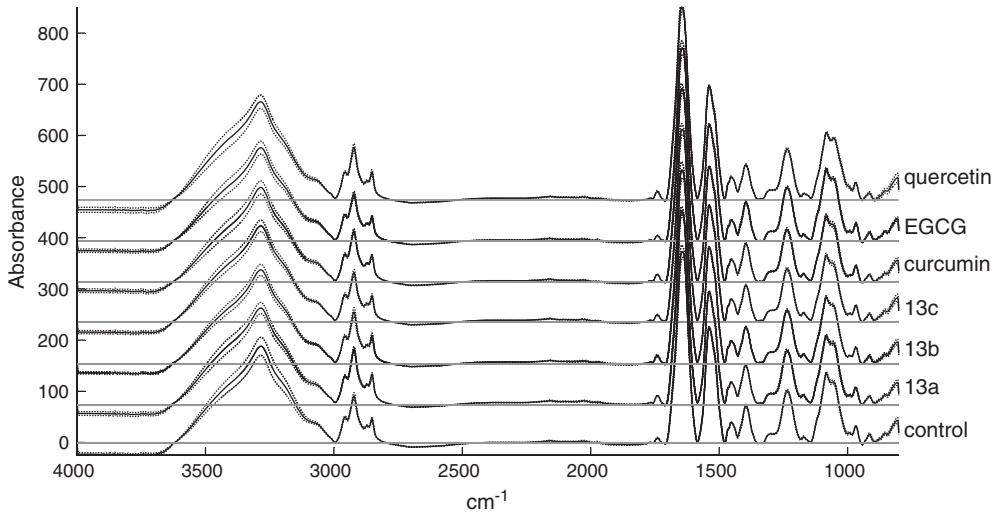

Fig. 2. Mean spectra (solid lines) ± standard deviation (dotted lines) of T98G cells exposed to the drug indicated in the right margin during 24 h at a concentration equal to its IC_{50}. Between 18 and 27 spectra were recorded for each condition. Original values of maximal absorbance ranged between 0.2 and 0.4 A.U. for all the spectra. Spectra were normalized for an equal area between 1582 and 1492 cm^{-1} and baseline corrected. For better readability, mean spectra were offset along the absorbance axis and presented on the same scale. The horizontal gray lines indicate the zero value for each spectrum.

at 2 h (Fig. 3A) and 6 h (Fig. 3B) are not identical. On Fig. 3A, two main groups are observed: one with the 3 synthetic molecules and the other with the natural polyphenols. After 6 h incubation, while the 3 synthetic molecules are still clustered together, curcumin is not grouped with the other natural compounds.

3.4. Principal component analysis and MANOVA

PCA statistical analyses on all individual spectra are reported in Fig. 4 with respect to each exposure time, i.e. 2 h (Fig. 4A and B), 6 h (Fig. 4C) and 24 h (Fig. 4D). Every point (star) in the plot from Fig. 4A is the projection of one of the original spectrum. The different molecules are identified by a unique color. In Fig. 4B, 95% confidence ellipses were drawn around the mean position of each cluster indicated by a square for each group. For the sake of clarity, 95% confidence ellipses around the mean position of each cluster are drawn for 6 h (Fig. 4C) and 24 h (Fig. 4D). PCA is a common statistical method used to analyze FTIR spectral data. However, it appears from Fig. 4 that differences are not very significant for most couples of molecules in the 2-dimensional representation as 95% confidences ellipses largely overlap, especially for 2 and 6 h (Fig. 4B and C). Yet, it must be considered that the 2 dimensional representation of the score plot describes less that 70% of the total variance. In order to test the significance of the full data, score values on the first 6 PCs, representing more than 99% of the variance, were submitted to MANOVA. Tables 3A–3C shows the result of MANOVA analyses carried out to investigate potential

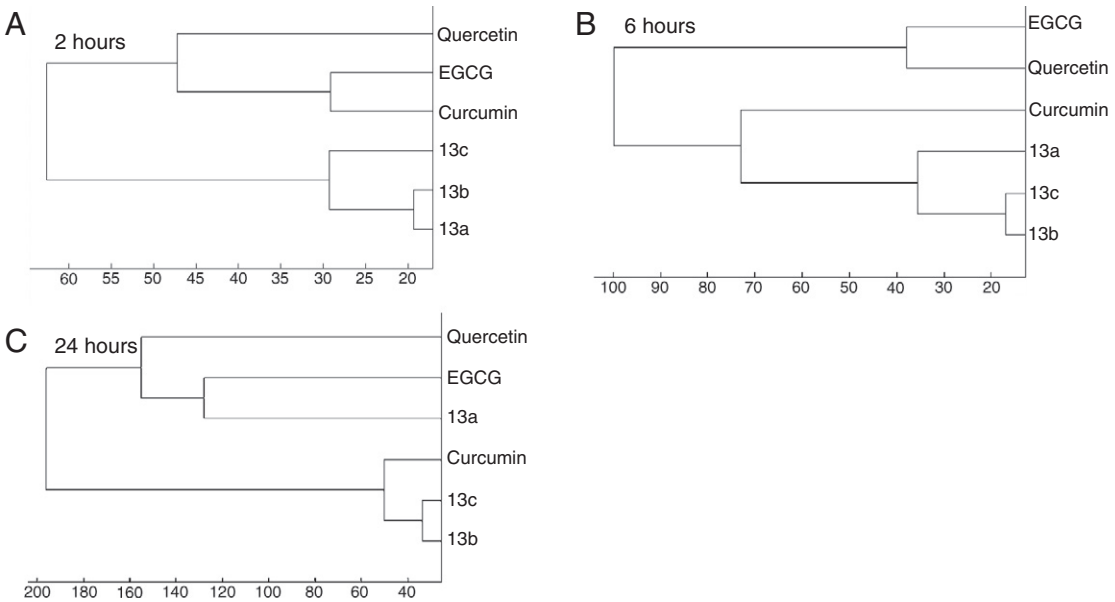

Fig. 3. Hierarchical classification of "the difference spectra" computed as the differences between mean spectra for T98G cells exposed to polyphenols and control cells for 2 h incubation (A), 6 h incubation (B) and 24 h incubation (C). The spectral range used for this analysis is 3000–2800 cm^{-1}, 1800–1700 cm^{-1} and 1600–1000 cm^{-1}.

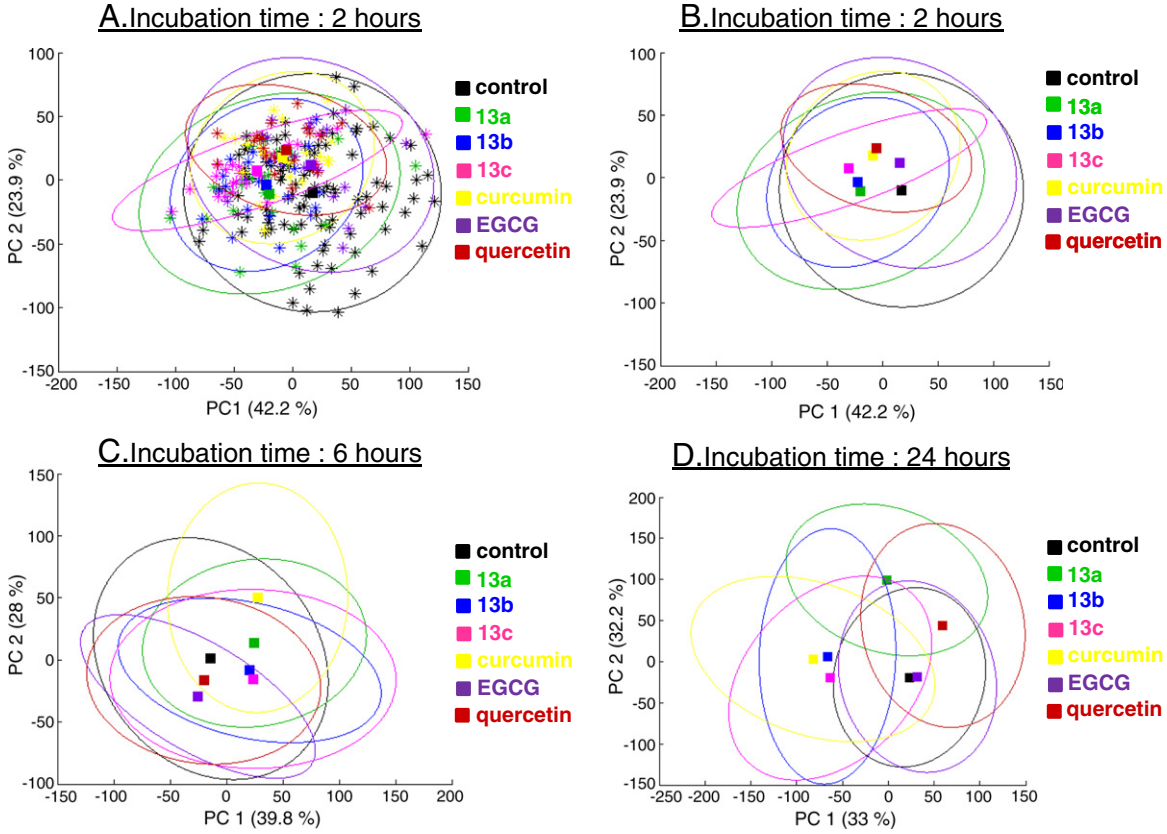

Fig. 4. Principal component analysis scores on PC1 and PC2 computed for each incubation time including all drugs. The spectral range used for this analysis is 3000–2800 cm^{-1}, 1800–1700 cm^{-1} and 1600–1000 cm^{-1}. Projection of spectra arising from untreated cells and those exposed to the drug during: A and B: 2 h, C: 6 h and D: 24 h. The different molecules are identified by a unique color as indicated on the legend, and 95% confidence ellipses around the mean position of each cluster were computed. The square is the position of the mean. Panel A illustrates the distribution of each 95% ellipses with respect to its respective cluster of points: each star represents the projection of one spectrum. Then, for a better readability, points have been erased and only ellipses are drawn on panels B, C and D.

differences between the 6 polyphenols in the space defined by the first six principal components. It can now be observed that statistically significant differences are evidenced for most couples of molecules.

The data in Tables 3A–3C indicate that 2 and 6 h of treatment with all molecules except EGCG induced significant modifications in T98G glioma cell metabolism. **13b** and **13c** do not show significantly different consequences for any incubation time.

3.5. Incremental Student t-tests

Insight into the chemical origin of the spectral modification appearing as a function of the incubation time for each polyphenol was obtained by subtracting i) the FTIR spectra of control (untreated) from 2 h-treated, ii) of 2 h-treated from 6 h-treated, and iii) of 6 h-treated from 24 h-treated ones. At each wavenumbers, a Student *t*-test was performed to assess the significance of the change. Results are reported in Fig. 5A (**13a**), 5B (**13b**), 5C (**13c**), 5D (curcumin), 5E (EGCG) and 5F (quercetin). Positive and negative peaks are representative of chemical groups respectively more or less abundant in the cells after exposure to the drugs. Thicker curves indicate wavenumbers where the absorbance are significantly different between two conditions (Student *t*-test, $\alpha = 1\%$). Interestingly, during the first 2 h of treatment and with respect to the majority of the drugs, limited but significant changes arise around 1050 and 1085 cm^{-1}, which are respectively characteristic of the C–O from carbohydrates and of phosphodiesters, mainly from nucleic acids [36–38]. A few significant wavenumbers also appear around 1740 cm^{-1}. These differences could be due to changes in the ester C═O stretching of phospholipids [37] or to protonation of aspartic and glutamic acid. Between 2 and 6 h, the observed modifications for the three synthetic polyphenols and for EGCG are less marked than what is observed for the first 2 h of treatment (Fig. 5). Surprisingly, a reverse effect is noticed between 2 and 6 h for the absorption bands of the stretching vibration of CH_2 and

Table 3A
P-values calculated by multivariate analysis of variance (MANOVA) on the first 6 principal components between each pair of treatment after 2 h incubation. Principal components were computed between 3000 and 2800 cm^{-1}, 1800 and 1700 cm^{-1} and 1600 and 1000 cm^{-1}, the scores on the first 6 principal components of all the spectra (between 18 and 27 spectra) for each compound were submitted to MANOVA.

P-values	Control	13a	13b	13c	Curcumin	EGCG	Quercetin
Control							
13a	$3.57\,10^{-8}$						
13b	$8.36\,10^{-7}$	$2.05\,10^{-5}$					
13c	$3.04\,10^{-7}$	$3\,10^{-4}$	0.0104				
Curcumin	$1.29\,10^{-12}$	$2.24\,10^{-8}$	$6.74\,10^{-12}$	$1.49\,10^{-10}$			
EGCG	0.0755	$9361\,0^{-9}$	$1.12\,10^{-5}$	$6.51\,10^{-6}$	$5.98\,10^{-11}$		
Quercetin	$3.76\,10^{-6}$	$2.04\,10^{-6}$	$4.93\,10^{-5}$	$9.45\,10^{-5}$	$5.07\,10^{-8}$	0.0082	

Table 3B
P-values calculated by multivariate analysis of variance on the first 6 principal components between each pair of treatment after 6 h incubation, conditions as in Table 3A.

P-values	Control	13a	13b	13c	Curcumin	EGCG	Quercetin
Control							
13a	$3.97\,10^{-8}$						
13b	$3.55\,10^{-7}$	$1.31\,10^{-5}$					
13c	$7.11\,10^{-9}$	$6.72\,10^{-7}$	0.11				
Curcumin	$6.66\,10^{-16}$	$5.73\,10^{-6}$	$1.6\,10^{-10}$	$3.07\,10^{-9}$			
EGCG	0.0136	$3.17\,10^{-11}$	$3.13\,10^{-8}$	$3.62\,10^{-6}$	$1.96\,10^{-13}$		
Quercetin	$4.34\,10^{-10}$	$1.73\,10^{-13}$	$1.61\,10^{-9}$	$1.27\,10^{-6}$	$1.55\,10^{-15}$	$1.02\,10^{-8}$	

CH_3 (3000–2800 cm^{-1}) mostly contained in the lipid acyl chains [38]. Finally, between 6 and 24 h, a large amplification of the effects detected earlier occurred.

4. Discussion

Polyphenolic compounds exhibit very complex mechanisms when exerting their anticancer effects, even *in vitro*. As illustrated in Table 1, they interfere with many biochemical pathways, which regulate various biological processes frequently involved in cancer cell biology. Until now, the exact mode of action of these molecules is not yet resolved. Thus, a global and rationale approach would be helpful to identify those polyphenols that display similar mechanisms of action versus those that display distinct ones in order to identify those polyphenols that could be further developed at the pre-clinical level, and then at the clinical one [4]. In this article we exploited FTIR spectra of glioma cells exposed to various polyphenols to obtain a signature of all the metabolic changes induced by these molecules and variations in the cell chemical content. The first question that can be addressed here is how robust is the FTIR approach.

FTIR analysis is based on the absorption of infrared light by vibrational transitions in covalent bonds and monitors the global chemical composition of the sample. A spectrum of cells is a superimposition of spectra of all cell constituents [39]. Furthermore, the IR spectra account not only for the chemical nature of cell molecules but also for their conformations and are, in particular, very sensitive to protein secondary structure [40]. Various applications have demonstrated the accuracy of this sum of information. In the 1980s, it was demonstrated that IR spectra of bacteria allow phylogenetic classification as accurate as the one built with current phylogeny techniques. The specific fingerprints obtained with IR spectroscopy led also to the identification of new species of bacteria [41,42]. This approach was also used in hundreds of applications, in particular to study eukaryotic cells. Changes between normal and cancerous cells were observed for various types of cancers by Fourier transform infrared (FTIR) spectroscopy [43,44]. Moreover, several recent experiments have evidenced that drug-induced metabolic disorder yield to a unique spectral fingerprint characteristic of the "mode of action" of the agent under investigation and should be amenable to classification similar to the ways bacteria gender, species, and strains can be classified [45]. Distinct effects of anticancer cardiotonic steroids on a prostate cancer cell line (PC-3) could be distinguished by FTIR spectroscopy [46]. Recently, 7 well-described anticancer drugs belonging to 3 different classes were tested on one cell line and drugs known to induce similar types of metabolic disturbances appeared to cluster together when the spectrum shapes were analyzed [28]. Finally, Draux et al. also demonstrated that spectral modifications induced by gemcitabine could be associated with drug concentrations and exposure times [47].

FTIR spectroscopy has also been successfully applied to obtain the IR signature of cell differentiation processes [48], cell cycle phases [49] and cell apoptosis [50,51]. So, spectral modifications caused by various events in the cell life have already been pointed out. In this work, as non-adherent cells have been eliminated prior to cell collection (see Materials and methods) only the adherent, i.e. living cells, were analyzed, suggesting that the spectral differences observed were not related to apoptosis. On the other hand, contribution of cell cycle-related spectral signature is 1) of very weak intensity with respect to the observed differences (Fig. 5) and 2) is negligible after 2 h incubation as it takes much more time to accumulate the bulk of the cells from G_0/G_1 into a later phase (unpublished observations). Yet, spectral changes observed after 2 h are particularly intense further ruling out the presence of a significant contribution of cell cycle arrest on the spectra.

In general, as FTIR response depends on the mass of the molecules, in most papers published in the literature, changes in the IR spectra of cells induced by a treatment have been monitored after a drug exposition of at least 12 h (or more). In the current work, spectral changes could be revealed as early after the addition of the drugs as 2 h. A stringent Student *t*-test ($\alpha = 1\%$) was performed to confirm the statistical significance of the difference at a several series of wavenumbers. Furthermore, as a control, we carried out the same Student *t*-test with two groups of spectra randomly selected among the untreated cells. A completely flat "difference spectra" with nearly no significantly different spectral regions was obtained. This test was at least repeated three times with various random selections of untreated spectra. Finally, the p-values obtained with the MANOVA also indicate a high level of significance in the variations observed.

The molecular origin of the spectral differences is difficult to establish considering the large variety of molecules present in the cells. The potential contribution of the polyphenol molecules themselves is however a legitimate question. Yet, such a contribution of the drugs themselves has been ruled out previously in similar studies [52]. Indeed, as described in the experimental procedure, cells were washed three times before FTIR measurements and all the free polyphenols were thus removed. Nevertheless, one could consider that drugs could accumulate inside the cells and contribute to the infrared spectra. This hypothesis was rejected because 1) spectra of 10^{-4} M drug solution processed as the cell suspension did not display any significant contribution and, 2) the

Table 3C
P-values calculated by multivariate analysis of variance on the first 6 principal components between each pair of treatment after 24 h incubation, condition as in Table 3A.

P-values	Control	13a	13b	13c	Curcumin	EGCG	Quercetin
Control							
13a	$<\times 10^{-20}$						
13b	$<\times 10^{-20}$	$8.67\,10^{-13}$					
13c	$9\,10^{-16}$	$5.87\,10^{-12}$	0.0492				
Curcumin	$<\times 10^{-20}$	$4.16\,10^{-11}$	$1.85\,10^{-6}$	$2.13\,10^{-6}$			
EGCG	$8.7\,10^{-5}$	$5.55\,10^{-16}$	$5.13\,10^{-14}$	$6.08\,10^{-11}$	$9.21\,10^{-13}$		
Quercetin	$<\times 10^{-20}$	$1.11\,10^{-16}$	$1.05\,10^{-16}$	$1.49\,10^{-13}$	$3.2\,10^{-14}$	$5.81\,10^{-13}$	

actual spectra of drug molecules (recorded at 10^{-2} M) are completely different from the difference spectra, strongly suggesting that the drugs themselves do not contribute to the spectral variations observed.

4.1. Comparison of newly synthesized "13" compounds

Little is known about how these molecules act when displaying their anticancer effects, at least *in vitro* [53]. It is already known that **13c** decreases the activity of a panel of kinases implicated in the control of the actin cytoskeleton organization, while **13b** only weakly inhibited kinase activity and compound **13a** not at all [48]. These three trivanillates also displayed markedly distinct modifications of $[Ca2+]_i$ (intracellular calcium concentration) [48]. **13a** did not modify [Ca2+]i, while **13b** and **13c** induced a transient and a sustained increase in [Ca2+]i, respectively [48]. Previous experiments demonstrated that **13a** induced cytotoxic effects in cancer cells, while **13b** and **13c** induced cytostatic ones [11,48]. The current data relating to FTIR-related data analyzed reveal that, indeed, **13b** and **13c** induce similar metabolic changes in T98G glioma cells after all incubation times, while **13a** induce markedly distinct metabolic modifications when compared to **13b** and **13c** (Table 3C and

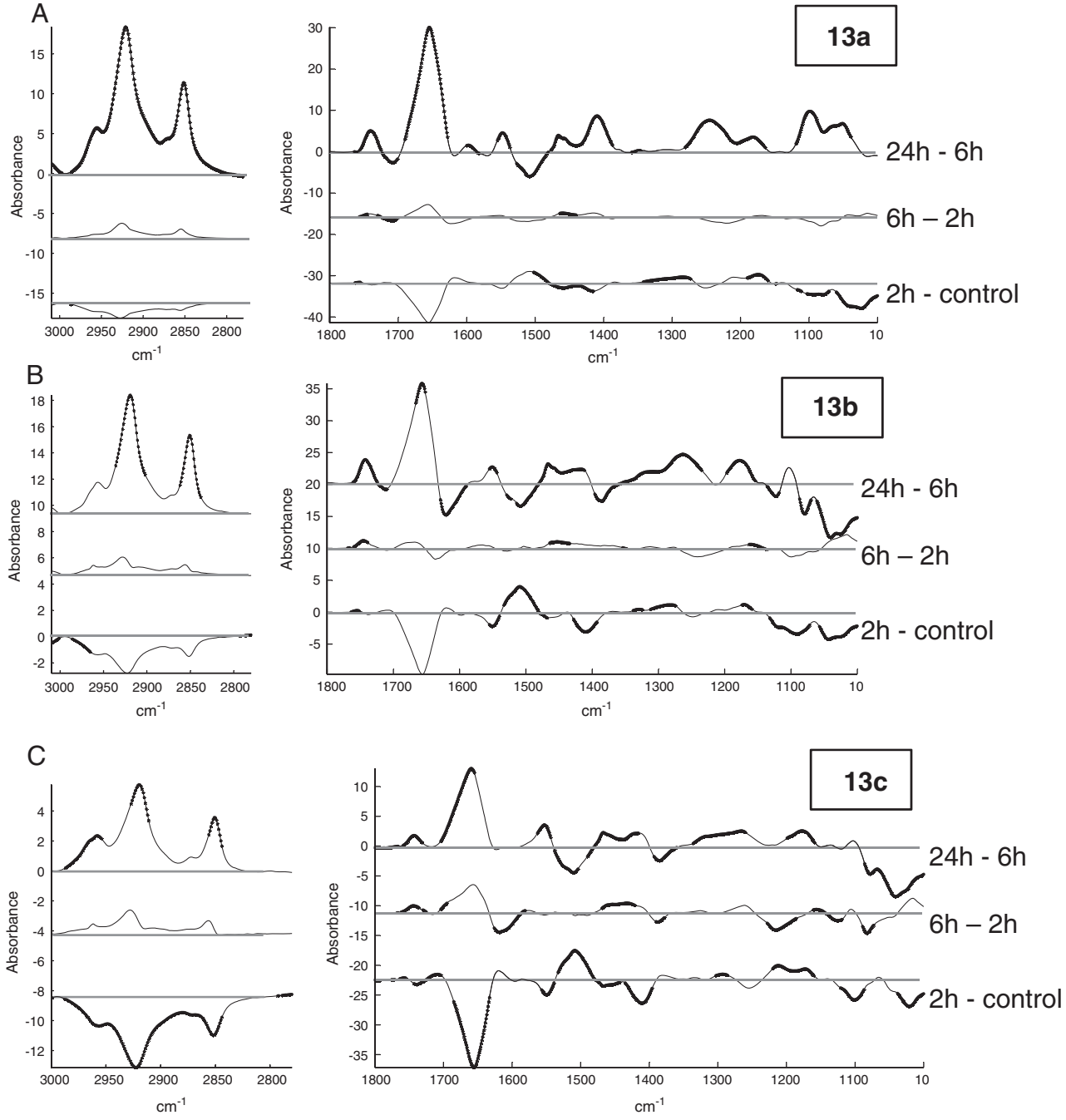

Fig. 5. Incremental Student *t*-test. Each spectrum is the difference between two average spectra obtained from successive pairs of experimental conditions. Spectra are offset along the absorbance axis for easier readability. The same scale was applied for all the spectra. The horizontal gray lines indicate the zero value for each spectrum. Thicker lines indicate wavenumbers statistically different ($\alpha = 1\%$) according to a Student *t*-test. Curves from the bottom to the top are difference spectra respectively calculated for 2 h-untreated cells, 6 h–2 h, 24 h–6 h. A: **13a**, B: **13**b, C: **13c**, D: curcumin, E: EGCG and F: quercetin.

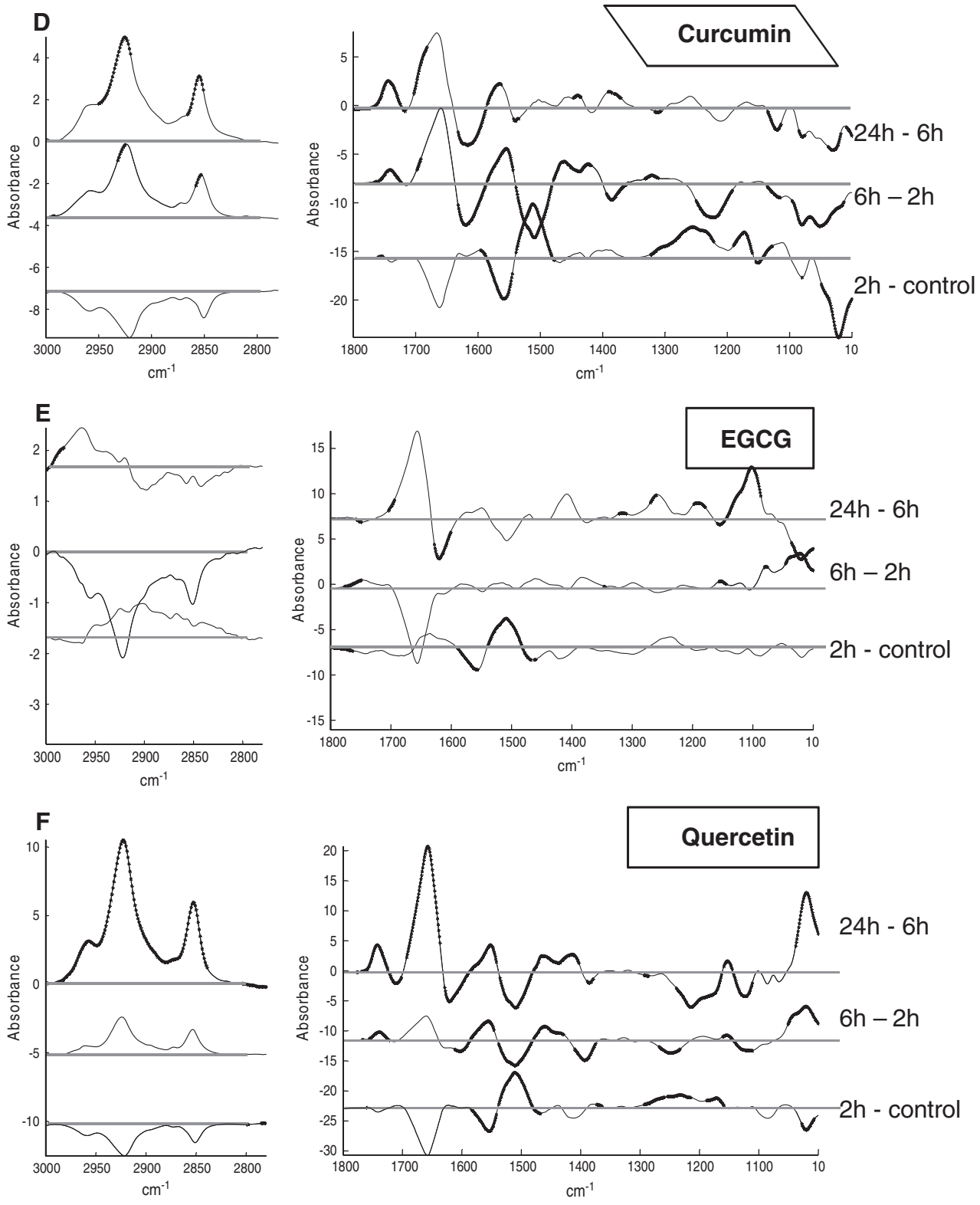

Fig. 5 (*continued*).

Fig. 3C). Altogether, these data thus indicate that FTIR analyses can identify unique cell response induced by very similar molecules and therefore could potentially help to avoid detailed investigations of compounds that display similar effects on cancer cell metabolism. It also reveals that curcumin is the closest natural polyphenol molecule in terms of global metabolic changes.

4.2. Incubation time

Exposure time appears to be a key experimental parameter when studying the mechanisms of polyphenolic compounds. A review by Ramos [10] already pointed out that experimental conditions including treatment length must be seriously considered because they can

determine the biological outcome. The current study indeed demonstrates that metabolic modifications induced by six polyphenols in T98G glioma cells markedly changed as a function of the time of exposure of T98G glioma cells to these polyphenols.

Interestingly, incremental Student *t*-test suggests that at least for the synthesized molecules **13**, larger changes appear between 0 and 2 h than between 2 and 6 h. Considerable changes appear when cells have been exposed to drugs during 24 h. It could be suggested that metabolic changes observed in the spectra at 2 h incubation, are more specific to the primary target affected and their first series of consequences. Spectral variations after longer exposure times might depict secondary biochemical consequences.

In conclusion, infrared spectroscopy is fast and cheap when compared with molecular biology approaches. This method provides an objective classifier of potential anticancer polyphenols according to their mode of action. It could therefore constitute a step of selection for the most promising molecules. The drawback of the method is that assignments to a particular molecule cannot be made. In spite of this limitation, infrared spectroscopy offers a good opportunity to obtain global information on drug signature because it measures simultaneously the lipidome, the proteome, the metabolome, etc.

Supplementary data to this article can be found online at http://dx.doi.org/10.1016/j.bbadis.2012.10.010.

Acknowledgements

This research has been supported by grants from the National Fund for Scientific Research (FRFC 2.4526.11 and 2.4533.10). E.G. and R.K. are Directors of Research with the “National Fund for Scientific Research”, Belgium. A.D. is a Research Fellow supported by the “National Fund for Scientific Research”, Belgium.

References

[1] C.S. Yang, J.M. Landau, M.T. Huang, H.L. Newmark, Inhibition of carcinogenesis by dietary polyphenolic compounds, Annu. Rev. Nutr. 21 (2001) 381–406.
[2] D. Lamoral-Theys, L. Pottier, F. Dufrasne, J. Nève, J. Dubois, A. Kornienko, et al., Natural polyphenols that display anticancer properties through inhibition of kinase activity, Curr. Med. Chem. 17 (2010) 812–825.
[3] S. Ramos, Effects of dietary flavonoids on apoptotic pathways related to cancer chemoprevention, J. Nutr. Biochem. 18 (2007) 427–442.
[4] S. Jagtap, K. Meganathan, V. Wagh, J. Winkler, J. Hescheler, A. Sachinidis, Chemoprotective mechanism of the natural compounds, epigallocatechin-3-O-gallate, quercetin and curcumin against cancer and cardiovascular diseases, Curr. Med. Chem. 16 (2009) 1451–1462.
[5] C.S. Yang, X. Wang, G. Lu, S.C. Picinich, Cancer prevention by tea: animal studies, molecular mechanisms and human relevance, Nat. Rev. Cancer 9 (2009) 429–439.
[6] S. Ramos, M. Alía, L. Bravo, L. Goya, Comparative effects of food-derived polyphenols on the viability and apoptosis of a human hepatoma cell line (HepG2), J. Agric. Food Chem. 53 (2005) 1271–1280.
[7] A.B. Granado-Serrano, M.A. Martín, L. Bravo, L. Goya, S. Ramos, Quercetin induces apoptosis via caspase activation, regulation of Bcl-2, and inhibition of PI-3-kinase/Akt and ERK pathways in a human hepatoma cell line (HepG2), J. Nutr. 136 (2006) 2715–2721.
[8] D.P. Chauhan, Chemotherapeutic potential of curcumin for colorectal cancer, Curr. Pharm. Des. 8 (2002) 1695–1706.
[9] L. Le Marchand, S.P. Murphy, J.H. Hankin, L.R. Wilkens, L.N. Kolonel, Intake of flavonoids and lung cancer, J. Natl. Cancer Inst. 92 (2000) 154–160.
[10] S. Ramos, Cancer chemoprevention and chemotherapy: dietary polyphenols and signalling pathways, Mol. Nutr. Food Res. 52 (2008) 507–526.
[11] D. Lamoral-Theys, L. Pottier, F. Kerff, F. Dufrasne, F. Proutière, N. Wauthoz, et al., Simple di- and trivanillates exhibit cytostatic properties toward cancer cells resistant to pro-apoptotic stimuli, Bioorg. Med. Chem. 18 (2010) 3823–3833.
[12] S. Reuter, S. Eifes, M. Dicato, B.B. Aggarwal, M. Diederich, Modulation of anti-apoptotic and survival pathways by curcumin as a strategy to induce apoptosis in cancer cells, Biochem. Pharmacol. 76 (2008) 1340–1351.
[13] J.D. Lambert, R.J. Elias, The antioxidant and pro-oxidant activities of green tea polyphenols: a role in cancer prevention, Arch. Biochem. Biophys. 501 (2010) 65–72.
[14] C. Chen, J. Zhou, C. Ji, Quercetin: a potential drug to reverse multidrug resistance, Life Sci. 87 (2010) 333–338.
[15] F. Branle, F. Lefranc, I. Camby, J. Jeuken, A. Geurts-Moespot, S. Sprenger, et al., Evaluation of the efficiency of chemotherapy in *in vivo* orthotopic models of human glioma cells with and without 1p19q deletions and in C6 rat orthotopic allografts serving for the evaluation of surgery combined with chemotherapy, Cancer 95 (2002) 641–655.
[16] B. Le Calvé, M. Rynkowski, M. Le Mercier, C. Bruyère, C. Lonez, T. Gras, et al., Long-term *in vitro* treatment of human glioblastoma cells with temozolomide increases resistance *in vivo* through up-regulation of GLUT transporter and aldo-keto reductase enzyme AKR1C expression, Neoplasia 12 (2010) 727–739.
[17] F. Lefranc, J. Brotchi, R. Kiss, Possible future issues in the treatment of glioblastomas: special emphasis on cell migration and the resistance of migrating glioblastoma cells to apoptosis, J. Clin. Oncol. 23 (2005) 2411–2422.
[18] F. Lefranc, V. Facchini, R. Kiss, Proautophagic drugs: a novel means to combat apoptosis-resistant cancers, with a special emphasis on glioblastomas, Oncologist 12 (2007) 1395–1403.
[19] B. Annabi, M.P. Lachambre, N. Bousquet-Gagnon, M. Page, D. Gingras, R. Beliveau, Green tea polyphenol (−)-epigallocatechin 3-gallate inhibits MMP-2 secretion and MT1-MMP-driven migration in glioblastoma cells, Biochim. Biophys. Acta 1542 (2002) 209–220.
[20] H. Jiang, L. Zhang, J. Kuo, K. Kuo, S.C. Gautam, L. Groc, et al., Resveratrol-induced apoptotic death in human U251 glioma cells, Mol. Cancer Ther. 4 (2005) 554–561.
[21] M. Rüweler, A. Anker, M. Gülden, E. Maser, H. Seibert, Inhibition of peroxide-induced radical generation by plant polyphenols in C6 astroglioma cells, Toxicol. *In Vitro* 22 (2008) 1377–1381.
[22] L.L. Zamin, E.C. Filippi-Chiela, P. Dillenburg-Pilla, F. Horn, C. Salbego, G. Lenz, Resveratrol and quercetin cooperate to induce senescence-like growth arrest in C6 rat glioma cells, Cancer Sci. 100 (2009) 1655–1662.
[23] J.C. Jeong, S.W. Jang, T.H. Kim, C.H. Kwon, Y.K. Kim, Mulberry fruit (*Moris fructus*) extracts induce human glioma cell death *in vitro* through ROS-dependent mitochondrial pathway and inhibits glioma tumor growth *in vivo*, Nutr. Cancer 62 (2010) 402–412.
[24] T. Mosmann, Rapid colorimetric assay for cellular growth and survival: application to proliferation and cytotoxicity assays, J. Immunol. Methods 65 (1983) 55–63.
[25] M.C. Alley, D.A. Scudiero, A. Monks, M.L. Hursey, M.J. Czerwinski, D.L. Fine, et al., Feasibility of drug screening with panels of human tumor cell lines using a microculture tetrazolium assay, Cancer Res. 48 (1988) 589–601.
[26] E. Goormaghtigh, V. Raussens, J.M. Ruysschaert, Attenuated total reflection infrared spectroscopy of proteins and lipids in biological membranes, Biochim. Biophys. Acta 1422 (1999) 105–185.
[27] A. Gaigneaux, C. Decaestecker, I. Camby, T. Mijatovic, R. Kiss, J.M. Ruysschaert, et al., The infrared spectrum of human glioma cells is related to their *in vitro* and *in vivo* behavior, Exp. Cell Res. 297 (2004) 294–301.
[28] A. Derenne, R. Gasper, E. Goormaghtigh, The FTIR spectrum of prostate cancer cells allows the classification of anticancer drugs according to their mode of action, Analyst 136 (2011) 1134–1141.
[29] E. Goormaghtigh, FTIR Data Processing and Analysis Tools, in: A. Barth, P.I. Haris (Eds.), Adv. Biomed. Spectrosc., vol. 2, 2009, pp. 104–128.
[30] E. Goormaghtigh, J. Ruysschaert, Subtraction of atmospheric water contribution in Fourier transform infrared spectroscopy of biological membranes and proteins, Spectrochim. Acta 50 (1994) 2137–2144.
[31] R.A. Johnson, D.W. Wichern, Principal components, in: Applied Multivariate Statistical Analysis, 4th ed., Prentice Hall, Upper Saddle River, 1998, pp. 458–513.
[32] H.E. Johnson, A.J. Lloyd, L.A.J. Mur, A.R. Smith, D.R. Causton, The application of MANOVA to analyse *Arabidopsis thaliana* metabolomic data from factorially designed experiments, Metabolomics 3 (2007) 517–530.
[33] J. Joe, H. Ward, Hierarchical grouping to optimize an objective function, J. Am. Stat. Assoc. 58 (1963) 236–244.
[34] R.A. Johnson, D.W. Wichern, Clustering methods and ordination, in: Applied Multivariate Statistical Analysis, 4th ed., Prentice Hall, Upper Saddle River, 1998, pp. 726–799.
[35] R. Gasper, E. Goormaghtigh, Effects of the confluence rate on the FTIR spectrum of PC-3 prostate cancer cells in culture, Analyst 135 (2010) 3048–3051.
[36] M. Diem, S. Boydston-white, L. Chiriboga, Infrared spectroscopy of cells and tissues: shining light onto a novel subject, Appl. Spectrosc. 53 (1999) 148A–161A.
[37] P. Lasch, A. Pacifico, M. Diem, Spatially resolved IR microspectroscopy of single cells, Biospectroscopy (2002) 335–338.
[38] D. Naumann, Infrared spectroscopy in microbiology, in: R.A. Meyers (Ed.), Encyclopedia of Analytical Chemistry, John Wiley & Sons Ltd., 2000, pp. 102–131.
[39] S. Boydston-white, T. Gopen, S. Houser, J. Bargonetti, M. Diem, Infrared spectroscopy of human tissue. V. Infrared spectroscopic studies of myeloid leukemia (ML-1) cells at different phases of the cell cycle, Biospectroscopy 5 (1999) 219–227.
[40] E. Goormaghtigh, V. Cabiaux, J.M. Ruysschaert, Determination of soluble and membrane protein structure by Fourier transform infrared spectroscopy. III. Secondary structures, Subcell. Biochem. 23 (1994) 405–450.
[41] D. Helm, H. Labischinki, G. Schallen, D. Naumann, Classification and identification of bacteria by Fourier-transform infrared spectroscopy, J. Gen. Microbiol. 137 (1991) 69–79.
[42] D. Naumann, D. Helm, H. Labischinski, Microbiological characterizations by FT-IR spectroscopy, Nature 351 (1991) 81–82.
[43] M.A. Cohenford, B. Rigas, Cytologically normal cells from neoplastic cervical samples display extensive structural abnormalities on IR spectroscopy: implications for tumor biology, Proc. Natl. Acad. Sci. U. S. A. 95 (1998) 15327–15332.
[44] B.R. Wood, M.A. Quinn, B. Tait, M. Ashdown, T. Hislop, M. Romeo, et al., FTIR microspectroscopic study of cell types and potential confounding variables in screening for cervical malignancies, Biospectroscopy 4 (1998) 75–91.
[45] R. Gasper, J. Dewelle, R. Kiss, T. Mijatovic, E. Goormaghtigh, IR spectroscopy as a new tool for evidencing antitumor drug signatures, Biochim. Biophys. Acta 1788 (2009) 1263–1270.

[46] R. Gasper, T. Mijatovic, A. Bénard, A. Derenne, R. Kiss, E. Goormaghtigh, FTIR spectral signature of the effect of cardiotonic steroids with antitumoral properties on a prostate cancer cell line, Biochim. Biophys. Acta 1802 (2010) 1087–1094.
[47] F. Draux, P. Jeannesson, C. Gobinet, J. Sule-Suso, J. Pijanka, C. Sandt, et al., IR spectroscopy reveals effect of non-cytotoxic doses of anti-tumour drug on cancer cells, Anal. Bioanal. Chem. 395 (2009) 2293–2301.
[48] C. Krafft, R. Salzer, S. Seitz, C. Ern, M. Schieker, Differentiation of individual human mesenchymal stem cells probed by FTIR microscopic imaging, Analyst 132 (2007) 647–653.
[49] H.-Y.N. Holman, M.C. Martin, E.A. Blakely, K. Bjornstad, W.R. Mckinney, IR spectroscopic characteristics of cell cycle and cell death probed by synchrotron radiation based Fourier transform IR spectromicroscopy, Biopolymers 57 (2000) 329–335.
[50] K.-zhi Liu, L. Jia, S.M. Kelsey, A.C. Newland, H.H. Mantsch, Quantitative determination of apoptosis on leukemia cells by infrared spectroscopy, Apoptosis 6 (2001) 269–278.
[51] U. Zelig, J. Kapelushnik, R. Moreh, S. Mordechai, I. Nathan, Diagnosis of cell death by means of infrared spectroscopy, Biophys. J. 97 (2009) 2107–2114.
[52] A. Derenne, M. Verdonck, E. Goormaghtigh, The effect of anticancer drugs on seven cell lines monitored by FTIR spectroscopy, Analyst 137 (2012) 3255–3264.
[53] D. Lamoral-Theys, N. Wauthoz, P. Heffeter, V. Mathieu, U. Jungwirth, F. Lefranc, et al., Trivanillic polyphenols with anticancer cytostatic effects through the targeting of multiple kinases and intracellular Ca(2+) release, J. Cell. Mol. Med. 16 (2011) 1421–1434.
[54] Y.J. Moon, X. Wang, M.E. Morris, Dietary flavonoids: effects on xenobiotic and carcinogen metabolism, Toxicol. *In Vitro* 20 (2006) 187–210.